# Formation of the Southland Current, New Zealand - a trajectory analysis

Alexandra Gronholz*[1], Mark Hadfield[2], André Paul[1], and Michael Schulz[1]

[1]*MARUM - Center for Marine Environmental Sciences and Department of Geosciences, University of Bremen, Germany*

[2]*National Institute of Water & Atmospheric Research (NIWA), Wellington, New Zealand*

August 31, 2016

**Abstract**

The formation of the Southland Current (SC) is investigated by the use of backward trajectories based on velocity fields of a regional ocean simulation. Modeled sea-surface temperatures and salinities are successfully validated. Furthermore, simulated trajectories are compared with drifter data. Afterwards, the SC formation is examined regarding the pathways of water parcels reaching the SC as well as regarding the source water masses forming the SC. Differences in the SC formation are found between summer and winter. During summer, water parcels that reach the SC in upper layers mainly origin from surface waters advected from the west. During winter, an increased amount of water parcels that end in SC surface layers origins from deeper layers at the west coast of the South Island of New Zealand, caused by upwelling at the western side of the Snares Shelf. Thus, results of this study may help to reconcile two so far contradictory views of SC water origin discussed in literature. Water parcels that reach the SC in deeper layers also differ during the seasons. During summer, water parcels are mainly transported around the Campbell

*Electronic address: agronholz@marum.de

Plateau whereas during winter, trajectories split between pathways around the plateau and across the plateau after entering on the eastern side of the plateau. The assessment of the total amount of Subantarctic (about 96 %) and Subtropical (about 4 %) water masses forming the SC in this study supports recent studies, by contradicting earlier work that see the SC as a mainly Subtropical current.

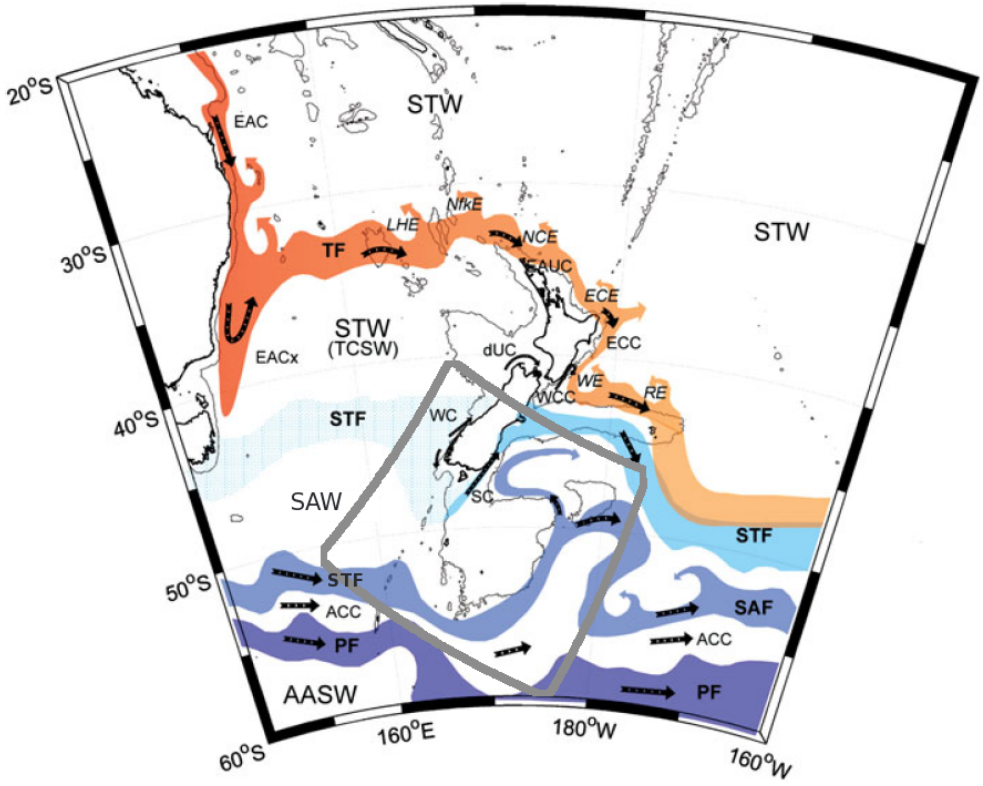


Figure 1: Overview of surface currents and fronts in the South-west Pacific ocean and applied ROMS domain in gray rectangle; modified from Chiswell et al. (2015); Antarctic Surface Water (AASW), Antarctic Circumpolar Current (ACC), d'Urville Current (dUC), East Australia Current (EAC), East Australia Current extension (EACx), East Auckland Current (EAUC), East Cape Current (ECC), East Cape Eddy (ECE), Lord Howe Eddy (LHE), North Cape Eddy (NCE), Norfolk Eddy (NfkE), Polar Front (PF), Rekohu Eddy (RE), Subantarctic Front (SAF), Southland Current (SC), Subtropical Front (STF), Tasman Front (TF), Tasman Sea Central Water (TSCW), Westland Current (WC), Wairarapa Coastal Current (WCC) and Wairarapa Eddy (WE)

# 1 Introduction

Along the eastern coastline of New Zealand's South Island a significant northwards current can be observed, the Southland Current (SC). The SC is associated with the Southland front (SF) (Fig. 1). This SF arises as part of the global Subtropical Front (STF) due to the local topographic conditions given by New Zealand, which interrupts the development of the global STF. As a result, the STF is shifted southwards and bends around the South Island. Several studies exist, that focus on the location of the STF and one discussion in literature, for instance, is whether the STF is located across the shelf south of New Zealand (Snares Shelf) or around the shelf and thus whether it is mainly

bathymetry formed or not (Smith et al., 2013). The STF separates warm and salty Subtropical water (STW) from cool and fresh Subantarctic water (SAW).

For a long time, the SC was supposed to be a mainly STW-transporting current (e.g. Jillett, 1969, Chiswell, 1996), while more recent studies suggest the main part of the SC to be of Subantarctic origin (Sutton, 2003).

In addition to the different assumptions regarding the source water masses forming the SC, a discussion regarding the location of origin of SC waters exist. While some studies suggest a flow from the western side of the South Island of New Zealand around the southern end of the island ending at the east coast in the SC (Heath et al., 1975), other studies state there is no connection between waters of the eastern and the western sides of the South Island of New Zealand and that SC waters are more likely advected zonally directly from the west across the Tasman Sea (Chiswell, 1996).

The SC is a very important feature as it influences the local as well as larger scale oceanography (Sutton, 2003) and it transports water into the subtropical convergence region near the Chatham Rise (e.g. Greig and Gilmour, 1992). Furthermore, measurements across SC sections, in particular water samples with subantarctic origin, are used to investigate parameters, such as $CO_2$ content and variation, in the context of climate change related questions (Currie et al., 2009).

This study aims to define the pathways of water parcels that reach the SC in certain depths to provide new information regarding the SC formation and thus also to provide an overview of the past of SC waters. Furthermore, it intends to estimate the amount of subtropical and subantarctic source water masses and the regions of their origin.

# 2 Methods and data

## 2.1 Ocean model setup

Velocity data for the trajectory model was taken from an ocean hydrodynamic model on a domain encompassing the continental shelf and deep ocean south of southern New Zealand (Fig. 2). The

model was the Regional Ocean Modelling System (ROMS), a free-surface oceanic model which uses the hydrostatic and Boussinesq approximations to solve the three-dimensional Reynolds-averaged Navier-Stokes equations on an Arakawa C grid with a terrain-following vertical coordinate (Shchepetkin and McWilliams, 2005, Haidvogel et al., 2008). The horizontal resolution of the grid varied from 2 km in the Southland Current area to 5 km at the boundaries; there were 30 layers in the vertical dimension. Lateral boundary data (velocity, temperature, salinity and sea-surface height) were taken from daily snapshots of the HYCOM GLBa08 global analysis and forecast system. The model used nudged radiative boundary conditions (Marchesiello et al., 2001). Model temperature and velocity in the interior were also nudged towards the HYCOM daily data in a 15-cell-wide zone adjacent to each boundaries, and at depth throughout the domain. The depth-dependent nudging rate was zero above 200 m and increased to 20 $d^{-1}$ at 800 m depth and below. The intention was to constrain the deep-ocean conditions with the HYCOM outer model but to allow the upper ocean to evolve freely. Surface stresses were calculated from 3-hourly winds from the NIWA-Econnect NZLAM 12 km atmospheric analysis and forecast system. The standard formula relating wind speed to surface stress involves a wind-speed-dependent term called the drag coefficient. For the present work this was calculated by the method of Smith (1988), however a comparison of preliminary model results with velocity measurements in the Southland Current indicated that wind-driven variability in the model was too low. The drag coefficient was therefore multiplied by a factor that was adjusted to optimize agreement: The final value chosen was 1.4. A similar adjustment has been found to be necessary in previous modelling exercises around New Zealand by M. Hadfield and colleagues and others (e.g. P. McComb pers. comm.). Heat and moisture fluxes through the sea surface were calculated using 6-hourly average data from the NCEP Reanalysis global atmospheric analysis system (Kalnay et al., 1996). The heat flux calculation included a correction term that caused the model sea-surface temperature (SST) to be nudged towards observed SST (the NOAA Optimum Interpolation 1/4° daily SST dataset, Reynolds et al. (2007)). The coefficient in the heat flux correction was 47 W $m^{-2}$ $K^{-1}$, which is sufficient to cause a 30 m thick surface mixed layer to relax towards the observed

SST with a time scale of 30 days. This prevents the modeled SST from departing too far from reality due to any biases in the surface fluxes, but has a negligible effect on day-to-day variability. The simulation was run from late 2007 to the end of 2012, with model analyses and trajectory calculations performed for the 5 years 2008 through 2012. The temporal resolution of the resulting data is 6 hours.

## 2.2 Observational data

### 2.2.1 Sub-surface temperature and salinity

For a validation of temperature and salinity fields, the CSIRO Atlas of Regional Seas (CARS) is used. CARS is a digital climatology of seasonal ocean water properties, produced by a combination of all (quality-controlled) available historical subsurface ocean property measurements. CARS2009, as used here, is a global dataset on a 1/2°resolution. For more information see Ridgway et al. (2002) and Dunn and Ridgway (2002).

### 2.2.2 Sea-surface temperatures

For the sea-surface temperature (SST) comparison, ROMS model results are compared with CARS2009 data, as described above, as well as with a 10-year mean (1993-2002) from the NIWA SST Archive (NSA), similar to the 5-year mean described by Uddstrom and Oien (1999) with a resolution of 6 km.

### 2.2.3 Ocean currents

Modeled currents are compared with measurements made with an acoustic Doppler current profiler (ADCP) installed at 170.847°E, 45.998°S from 22 June to 7 December 2009. The site is at 115 m depth on the continental shelf southeast of Otago Peninsula. The instrument returned vertical profiles of horizontal velocity every 30 minutes from approximately 20 m above the bottom to approximately 20 m below the surface.

Model velocity profiles were interpolated to the ADCP site from the ROMS simulation and saved at 30 minute intervals. Both the modeled and observed velocity profile data were then interpolated to a

common spacing (1 hour).

### 2.2.4 Global drifter program data

To validate the ocean model performance for the later application of the trajectory model, drifter data from the Global Drifter Program (GDP) are used. The GDP is the principle component of the Global Surface Drifting Buoy Array, a branch of the National Oceanographic and Atmospheric Administration (NOAA) Global Ocean Observing System (GOOS) and a scientific project of the Data Buoy Cooperation Panel (DBCP) (Pazos, 2015 and Lumpkin and Pazos, 2007). Currently, a global array of approximately 1250 drifters is available. Observational drifter data are provided for more than 15 years in the global oceans and include temperature and velocity fields as well as longitude and latitude information for an identification of the drifter's position in a 6-hourly resolution.

## 2.3 TracPy - Trajectory model

In this study, TracPy (Thyng and Hetland, 2014) is applied to simulate water parcel pathways. TracPy is a Python wrapping of the Fortran Lagrangian trajectory model TRACMASS, which has been applied to many atmospheric and oceanic general circulation models in the past. TRACMASS was originally developed by Döös (1995) and Blanke and Raynaud (1997) for stationary velocity fields and afterwards adapted by Vries and Döös (2001) for time-dependent velocity fields (Döös et al., 2011). TRACMASS offers the possibility to add additional explicit subgrid horizontal and vertical diffusion to the drifters pathway. In this study, no explicit subgrid horizontal diffusion is applied since the ROMS resolution of 2 km is expected to represent most of the important horizontal turbulent activity. For the vertical overturning a diffusion value of 0.1 $m^2\ s^{-1}$ is applied, as given by the mean vertical diffusivity of the ROMS simulation.

The basic elements of the above described TRACMASS trajectory model is wrapped in Python routines. This combination is called TracPy. TracPy offers the opportunity to run simulations in two (2D) or three (3D) dimensions. In the 2D case, vertical fluxes are not calculated but set to zero so

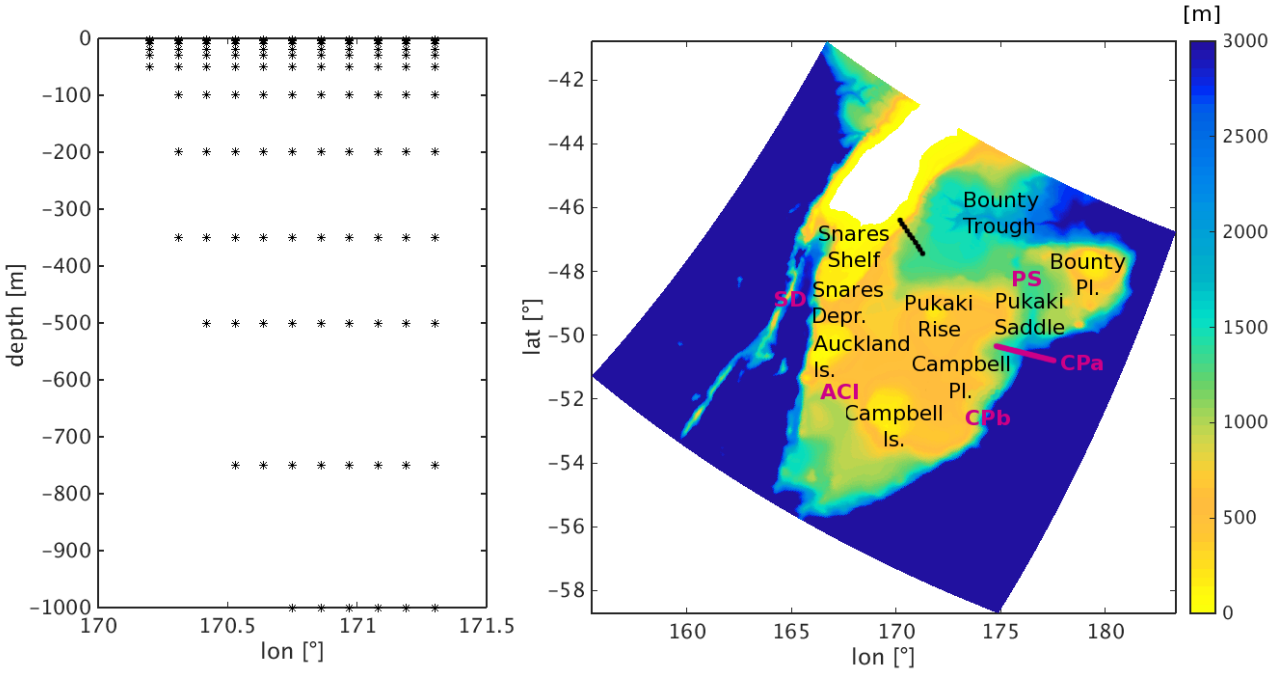


Figure 2: Distribution of the 119 simulated tracers (per time step) in different depths (left) over the Southland Current section (right, black dots) as defined by Fernandez (2016); different entrees of water masses as explained below in Sec. 3 given by: SD (Snares Depression), ACI (Auckland and Campbell Island), CPa/CPb (Campbell Plateau a and b) and PS (Pukaki Saddle); colors for bathymetry

that the drifter stays in its vertical position. For the validation in this study, which consists of a comparison of simulated trajectories with GDP data, a 2D simulation is conducted. For the general study later on, drifters are simulated in 3D. The starting location regarding longitude and latitude extension of the drifters in the 3D simulation is based on the study of Fernandez (2016), who defined the extension of the Southland Current between 1993 and 2012 from satellite data. Following this definition for the section, the drifters are placed in several depths: -2, -5, -10, -20, -30, -50, -100, -200, -350, -500, -750 and -1000 meters. In total, 119 drifters are distributed over this latitude/longitude extension and depths. Fig. 2 gives an overview of the drifter location.

### 2.4 Trajectory validation

As an additional mean to validate the ocean model performance, drifter data from the GDP are used. This trajectory validation follows the approach from Liu and Weisberg (2011), based on studies of

Price et al. (2006) and Barron et al. (2007). This approach to assess model performance is based on the so-called separation distances ($d$) between modeled and observed trajectories at a certain point of time after model initialization. The ultimate aim of this validation technique is to define a so-called trajectory model skill score ($ss$) which provides a number between 0 and 1 to assess whether the model performance is successful or not. To calculate the skill score, several calculation steps have to be done before. Differences inherent in predicting Lagrangian trajectories are compounded by errors in the simulated velocity fields (Barron et al., 2007). To reduce such errors, previous studies applied higher particle densities (Oezgoekmen et al., 2000) or other additional oceanographic data (Paldor et al., 2004). To get an appropriate estimate of the model performance by solely using the given Lagrangian trajectory information without an increased number of drifter trajectories or additional oceanographic data, first of all a non-dimensional index is defined as

$$s = \frac{\sum_{i=1}^{N} d_i}{\sum_{i=1}^{N} l_{oi}} \tag{1}$$

with $N$ as number of total time steps, $d_i$ as separation distance at time $t_i$ and $l_{oi}$ as lengths of the observed trajectory at that point of time. Thus, $s$ can be seen as an index that weights the separation distances ($d$) by the lengths of the observed trajectories ($\mathrm{l}_o$), both cumulatively. No additional information are needed. Both, the GDP as well as the TracPy trajectories are dynamic in time. The calculation of $s$ (Eq. 1), which uses several comparisons during the trajectories' pathways, takes this independent dynamics into account. It even recognizes if trajectories are deviating (converging) somewhere in the middle of their pathways but later on converge (deviate) again. Otherwise, by the use of the corresponding endpoints solely, in such a case the error would be underestimated (overestimated). Once this normalized cumulative separation distance, $s$, is defined, the skill score ($ss$) is defined as

$$ss = \begin{cases} 1 - \frac{s}{n} & (\mathrm{s} \leq \mathrm{n}) \\ 0 & (\mathrm{s} > \mathrm{n}) \end{cases} \tag{2}$$

where $n$ is a tolerance threshold, a non-dimensional number that defines the requirements or what is defined to be a successful performance. $ss = 0$ means the model has no skills. $ss = 1$ means it is performing in an ideal, perfect way. For the definition of $n$, this study follows Liu and Weisberg (2011) who take $n = 1$ as a reasonable choice. The smaller the $n$-value the stricter the requirements for the definition of a successful model performance.

The TracPy drifters are simulated in a 2D simulation to imitate the GDP drifter's behavior. All GDP drifter located in the entire ROMS domain are taken into account for the validation to increase the sample size, instead of conducting a validation that only focuses on the Southland Current (SC) region, as GDP drifters passing the SC are relatively rare. The drifters are initialized every 5 days. Previous studies showed that skill scores do not differ significantly for a release every 1, 2, 3, 4 or 5 days (Liu and Weisberg, 2011). Thus, every 5 days the positions of the GDP drifter inside of the domain are extracted from the dataset and a TracPy simulation is started at the same positions at the same time. Each started TracPy simulation is run for 30 days forward in time. Afterwards, the positions of GDP drifter and TracPy drifter are compared for each starting day after each simulation day up to 30 days of simulation. Results will be shown as an example for the comparison after 1, 3, 5, 10, 20 and 30 days.

# 3 Results

## 3.1 ROMS validation

### 3.1.1 Sub-surface temperature

Sub-surface temperatures in 200 m depth are compared between CARS2009 climatology data and model results (Fig. 3). ROMS data are interpolated to the CARS2009 grid points and a point-by point comparison is conducted. A statistic analysis of the differences between the datasets (ROMS - CARS2009) gives a mean of -0.09, a root-mean-square of 0.32, a standard deviation of 0.31 and a correlation coefficient of 0.98. The comparison shows a good overall agreement, with very little bias

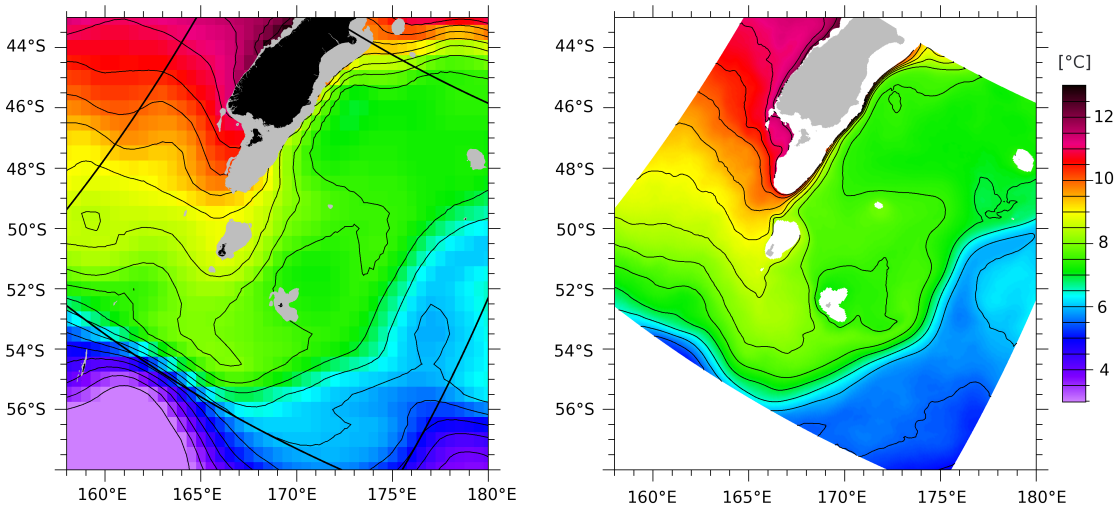


Figure 3: Comparison of sub-surface temperatures between climatology data (left) and model results (right) between 2008 and 2012

and a high correlation indicating that all the major features are represented successfully in the model simulation. The major difference can be found in the much sharper fronts in the model simulation. This applies to the Southland Front along the eastern edge of Snares Plateau as well as the Southland Otago shelf and also to the Subantarctic Front along the southeast edge of Campbell Plateau. The SST comparison below suggests that the sharper fronts in the model are realistic, and the smoothed-out fronts in the CARS2009 data result from the relatively large smoothing radius, which is approximately 250 km in this area, see Fig. 6 in Ridgway et al. (2002).

### 3.1.2 Sub-surface salinity

The comparison between climatology data (CARS2009) and the simulations in 200 meters depth (Fig. 4) shows an appropriate representation of the Subantarctic Front as well as the Southland Current region. Contour lines follow similar structures. Nevertheless, salinity values in the north of the domain tend to be slightly lower in the simulation compared to climatological data. Anyway, it should be mentioned again, that the CARS2009 climatology only includes data until 2008 whereas the simulation is run from 2008 to 2012. In the meanwhile, a newer Argo-only version is available which is frequently

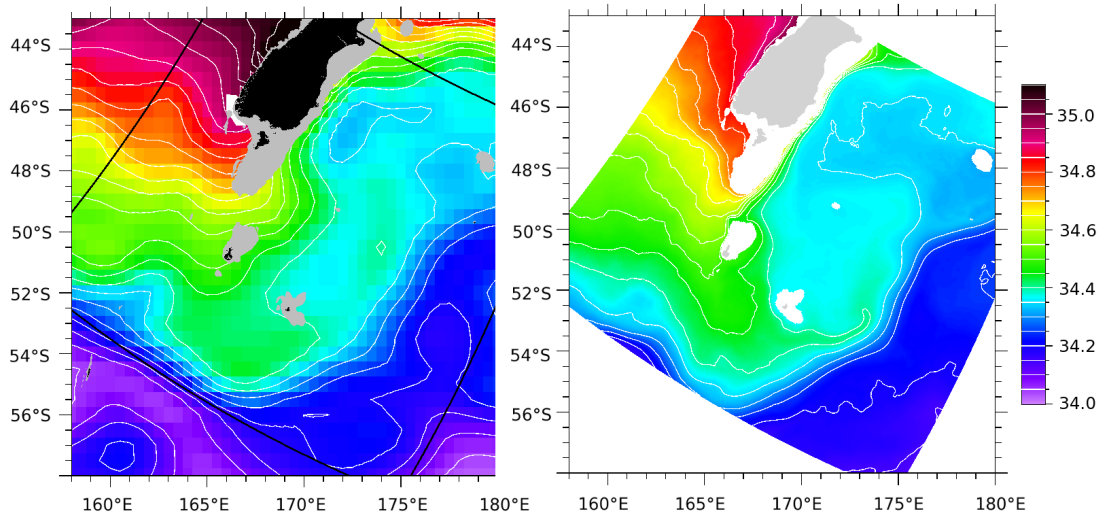


Figure 4: Comparison of 200 meter salinity between climatology data (left) and model results (right) between 2008 and 2012

updated. This dataset, however, cannot be used here, as Argo floats travel at 1000 m depth most of the time and thus cannot sample data in wide and important parts of the domain (over the shallower Campbell Plateau, for instance).

Differences have been calculated as described before, with the omission of a few (about 6) grid points with anomalously low salinity values in the model and the CARS dataset next to the Fiordland coast. Resulting statistics (ROMS - CARS2009) show a mean of -0.04, a root-mean-square of 0.08, a standard deviation of 0.07, and a correlation coefficient of 0.98. Similar to the sub-surface temperature comparison, the sub-surface salinity comparison shows a good overall agreement, pointing out much sharper fronts compared to the smoothed CARS2009 fronts.

### 3.1.3 Sea-surface temperatures

In addition to the sub-surface temperature validation above, SST also indicate a similar agreement. The comparison between sea-surface temperature data from CARS2009, the NIWA SST Archive (NSA) and the model results (Fig. 5) shows that the CARS2009 fields are smooth, as expected from the smoothing radius of about 250 km, and that the model is generating realistically sharp SST gradients

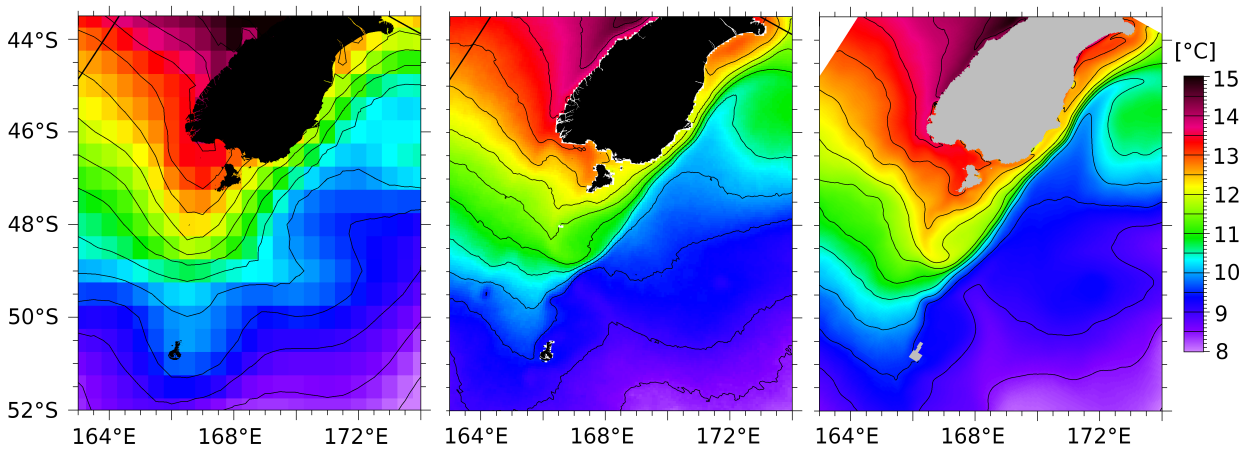


Figure 5: Comparison of sea-surface temperatures (SST) between observations (CARS2009, left), NIWA SST Archive (NSA, 1993 - 2002, middle) and model results (right)

at the Southland Front.

### 3.1.4 Ocean currents

In comparing the modeled and observed velocity profiles it is necessary to account for the fact that the model does not include tidal forcing, and therefore does not attempt to reproduce the tidal oscillations present in the observations. The observations were therefore low-pass filtered (the 51G113 filter from Thompson (1983), applied to hourly values) to remove the tidal component.

Fig. 6 shows a comparison of filtered velocity data from the ADCP and the model. In both the ADCP and model data, the velocities are clearly aligned along an axis at approximately 30° (clockwise from true north). The comparison here is based on data near the middle of the water column (ADCP level 5, 63 m below the surface). The figure illustrates the mean current and the variability about this mean in terms of the variance ellipse (Preisendorfer, 1988). Parameters that define the variance ellipses are listed in Tab. 1.

The agreement in the mean current indicates that the model supports a Southland Current of the correct strength. The good agreement in the semi-major axis has been achieved by adjusting the multiplier applied to the surface stresses used for forcing the model. To assess how accurately the modeled fluctuations in the currents match the observed fluctuations in time, Fig. 7 shows time

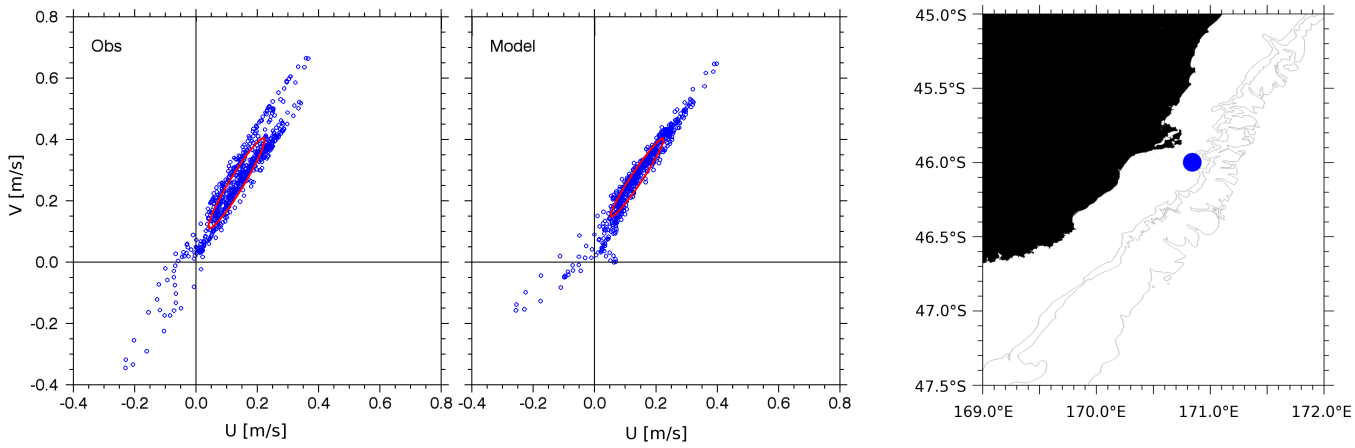


Figure 6: Comparison of filtered velocity data from the ADCP and the model, variance ellipse in red; ADCP location on the right (blue dot)

Table 1: Variance ellipse parameters based on hourly, detided velocity data at 63 m depth from ADCP and model simulation

| Parameter | Observations | Model |
|---|---|---|
| Mean magnitude [m $s^{-1}$] | 0.289 | 0.308 |
| Mean inclination [°] | 27.2 | 26.7 |
| Semi-major axis [m $s^{-1}$] | 0.172 | 0.153 |
| Semi-minor axis [m $s^{-1}$] | 0.024 | 0.019 |
| Ellipse inclination [°] | 31.3 | 33.7 |

series of the velocity component along the principal direction, taken here as 30°. The fluctuations in the model velocity (red) track those in the observations (blue) very well in magnitude and phase, as indicated by the correlation coefficient of 0.94 between the two series. A similar comparison for a direction at right angles to the principal direction shows a poorer match and consequently a lower correlation coefficient of 0.40 (see Fig. 8). The poorer performance in hindcasting fluctuations in this direction is understandable as these fluctuations represent relatively small deviations in the much stronger along-axis currents. Overall the comparison indicates that the model's representation of the mean flow and variability in the Southland Current is realistic.

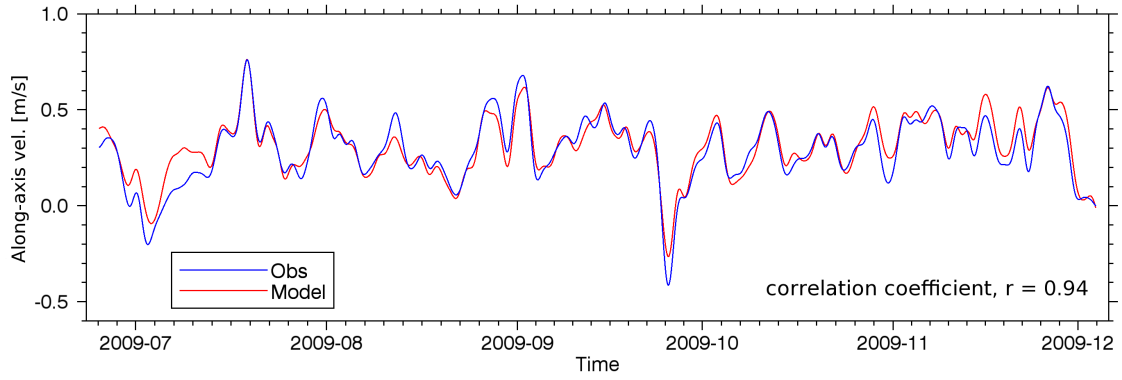


Figure 7: Comparison of along-axis model velocity (red) and observations (blue)

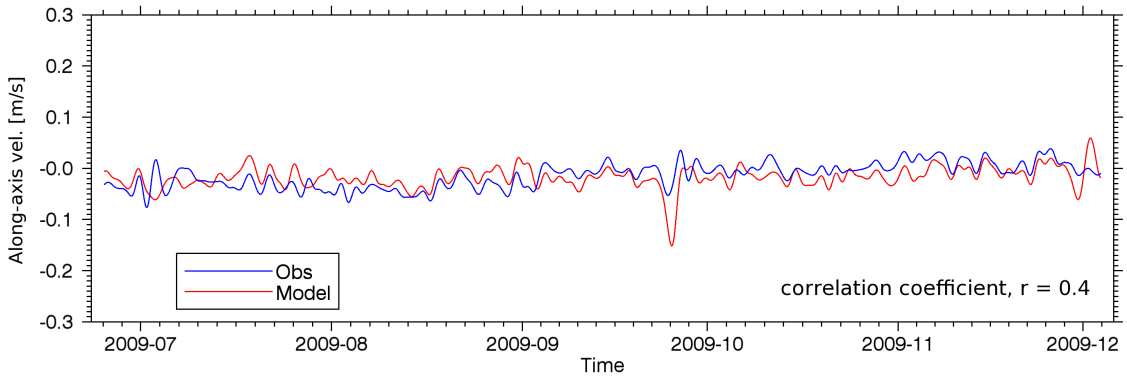


Figure 8: Comparison of across-axis model velocity (red) and observations (blue)

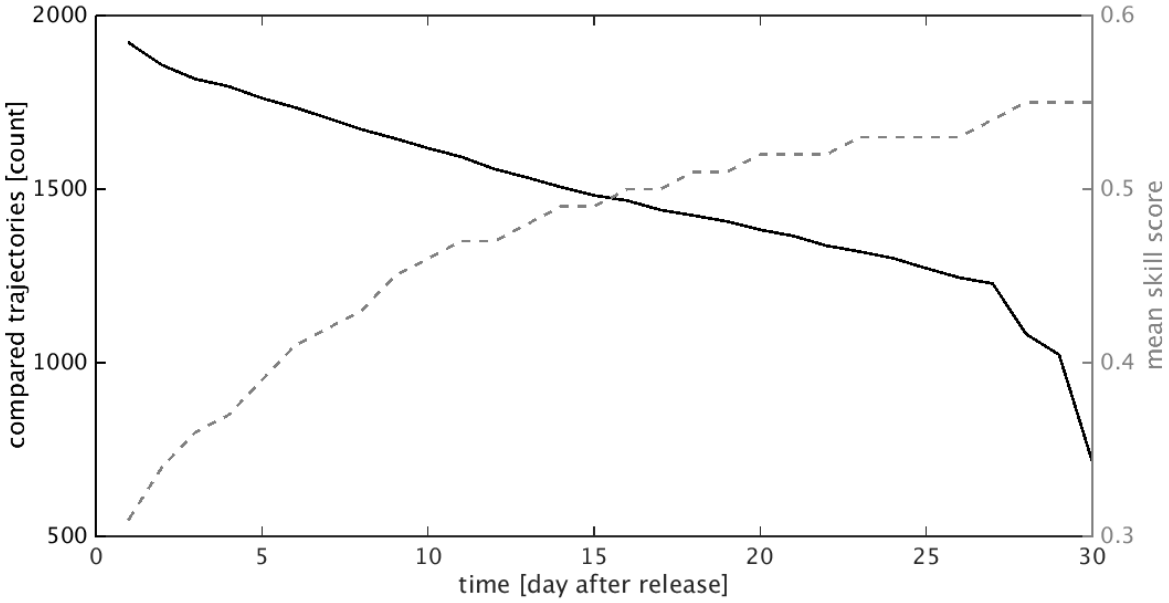


Figure 9: Overview of the number of compared trajectories (black) and the mean skill score ($mss$, dashed, gray) depending on the day after release

### 3.1.5 Trajectories

For the comparison of the simulated trajectories with observational drifter data, a large number of trajectories are compared within the years 2008 to 2012. The number of validated trajectories depends on the point of time after the release. For one day after the release, and thus one day after the simulation start, 1921 drifters are compared. During the simulation, several drifter leave the domain. Thus, the number of drifters decreases down to 715 (after 30 days of simulation). The number of compared trajectories as well as the mean skill scores ($mss$) for days 1 to 30 after release is given in Fig. 9. The skill scores show minimum values of 0.31 (after one day of simulation) and continuously increase with the length of the simulation to maximum values of 0.55 for 30 days after release. Figure 10 shows the frequency of occurrence of the normalized cumulative separation distance ($s$) after 3, 5, 10, 20, 25 and 30 days of release for the years 2008-2012. It illustrates the decreasing $s$-values with increasing simulation length. The smaller the $s$-value, the more skill the simulations have: $s$-values of zero are defined as 'perfect simulation' and $s \geq 1$ are defined as 'simulation with no skill' (see Sec. 2.4). Lower $s$-values, and thus higher skill-scores ($ss$), can be found the longer the simulation is. For

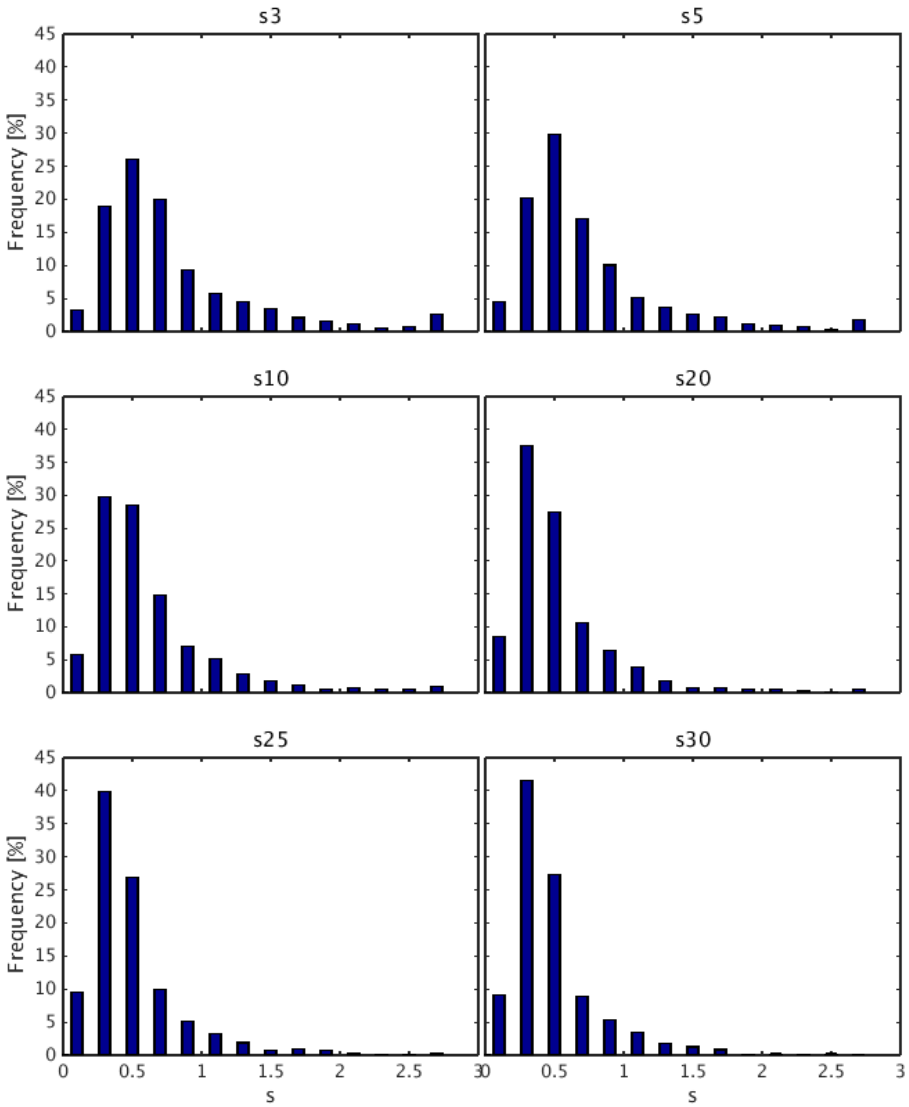


Figure 10: Frequency of occurrence of the normalized cumulative separation distance ($s$) after 3, 5, 10, 20, 25 and 30 days of release

days 1 to 5 after release, several $s \geq 1$ and even $\geq 2.7$ can be found. In contrast, after 25 or 30 days of simulation, almost no $s$-values $\geq 1.5$ occur anymore. Therefore, the occurrence of smaller $s$-values between 0.2 and 0.4 increases notably in the longer simulations from 18 % (after 3 days of simulation) to 42 % (after 30 days of simulation).

### 3.2 Backward trajectories

To investigate the water masses forming the Southland Current, two approaches are applied. First, the distribution and frequency of occurrence of the backward trajectories for the period 2008 to 2012 is investigated. Secondly, the water masses are defined at the end of each trajectory (after 70 days) by the determination of the salinity and temperature properties of the corresponding water parcel (Sec. 3.3). Fig. 11 gives an overview the first approach. From now onwards, the following terminology will be applied: The location on the SC section at which each back-trajectory originates will be called the 'destination point'. The path it follows is the 'back-trajectory' and the location at the end of this back-trajectory is defined as the 'source point'. Movement descriptions and directions are explained corresponding to a flow in reality (forward movement). A clear difference of the back-trajectories can be found for the different starting depths on the SC. A general tendency can be seen: The deeper the destination point of the water parcels had been, the stronger directly coming from the east is the resulting back-trajectoy. Or in other words, water parcels that reach deeper areas of the SC section tend to origin increasingly from source points in the (south-)east. Compared to that, water parcels reaching the upper water column (2 meters, 5 meters) arrive rather uniformly spread from all directions with a main direction from the south-west. Regarding destination points from 10 or 20 meters depth onwards, an increasing number of trajectories can be found that, in addition, build a clear track from the south in the east. This additional track becomes stronger with deeper destination points. From approximately 100 meters to 350 meters depth of the destination points, the back-trajectories start to form a rather tripartite behavior with three main directions: from the west (Fig. 2 entrance

SD for Snares Depression), straight from the south (Fig. 2 entrance ACI for Auckland and Campbell Island) and from the south in the east (Fig. 2 entrance PS for Pukaki Saddle). In 500 meters depth the back-trajectories from the west decrease notably and mainly the two pathways from the south (entrances ACI and PS) persist. In 750 meters depth the back trajectories from the west disappear completely and only the two pathways from the south remain, whereas in 1000 meters depth even the trajectories straight from the south vanish. In this depth, the flow is coming solely from the south in the east (entrance PS).

Comparing the different southern seasons of spring (September, October, November), summer (December, January, February), autumn (March, April, May) and winter (June, July, August), two main features of the trajectory pathways can be observed: 1. characteristics regarding the water parcels with destination points in the upper ocean, down to about 50 meters, as represented by the 2 meters destination point back-trajectories in Fig. 12 a & b, and 2. characteristics regarding the water parcels with destination points in the deeper layers, with a clear signal down to 500 meters and still slightly in 750 meters, as represented by the 200 meters back-trajectories in Fig. 12 c & d.

The following can be observed in the upper ocean: During winter time, back-trajectories show an increased amount of source-points along the western New Zealand shoreline and thus are coming rather from the north. They are following a strong bend around an area located south of the southern end of New Zealand followed by ascending south-eastwards of this area (see color transition from yellow to blue in the back-trajectory pathways in Fig. 12 b). This behavior can also be seen in the summary of all trajectories in Fig. 11 by the yellow u-shape (increased frequency) of the pathways, that appears at about 167 °E and 49 °S, which corresponds to entrance SD in Fig 2. These pathways are produced during winter time. In contrast to this, back-trajectories tend to arrive more straightly spread and uniformly from the west during summer time and they furthermore already origin from surface layers without ascending (Fig. 12 a). This can also be seen in Fig. 11 by the single spread most western back-trajectories and source-points at around 50 °S. Those trajectories are produced during summer time.

For destination points in the deeper layers, the following can be observed: As explained before, three entrances for water masses, that reach the SC section up to 500 meters, exist. These entrances can clearly be seen in Fig. 11 in 200 meters depth for instance. Comparing the seasonal behavior in these deeper layers it can be observed that during summer (Fig. 12, c) pathway PS is the most frequent one, also covering the longest travel distances, whereas during winter the transport through this pathway is reduced in frequency and strength and the main transport is therefore coming basically through the pathway further to the west. Investigating the more detailed illustration of the pathways in Fig. 12 d), the source points of the back-trajectories traveling from the direction of entrance ACI finally suggest a fourth entrance, which is shown in Fig. 2 by entrances CPa and CPb (for Campbell Plateau a and b). Pathway SD does not vary remarkably in these depths.

Additional test simulations for the assessment of general reproductivity and agreement of forward and backward trajectories regarding the applied subgrid diffusion are also carried out (not shown). For this purpose, trajectories are started on the SC transect, are simulated first backwards and resulting endpoints are used afterwards to start a forward simulation. Results show, that almost all drifters end again on the starting positions across the SC section, with only some deviations in some of the trajectories in the upper water column regarding the travel speed (some are a bit slower, some a bit faster). No tracer leaves the SC, all end as expected across the SC and the majority of about 90% even meets very well the original starting positions.

### 3.3 Water mass origin

In addition to the pathway information as described above, the properties of the source water masses are investigated to get information regarding the composition of the water reaching the SC section. The water reaching and forming the SC is assumed to originate from two different water mass types: warmer and saltier water with subtropical origin (SubTropical Water, STW) and colder and fresher water with subantarctic origin (SubAntarctic Water, SAW). When the water reaches the SC section it

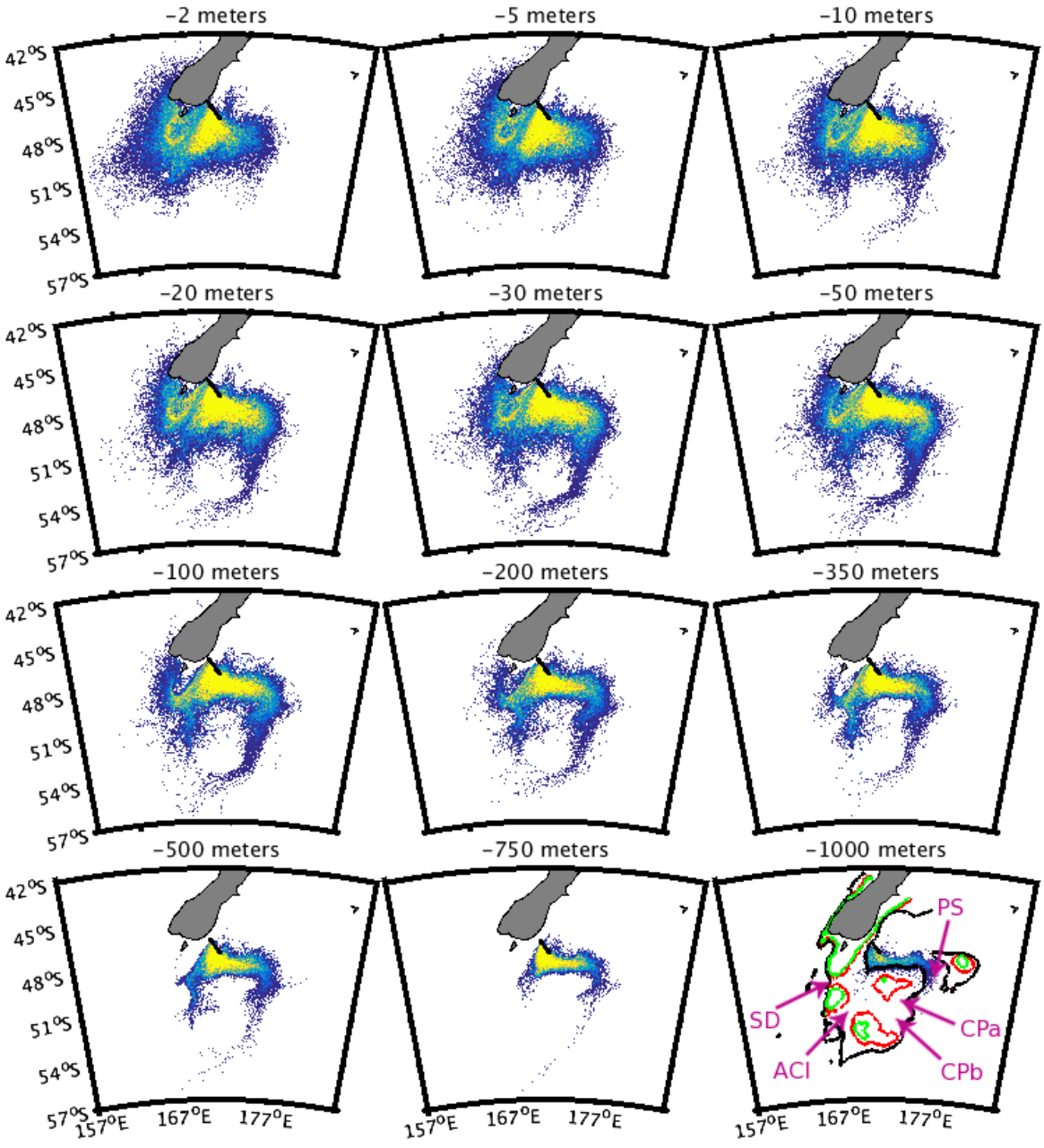


Figure 11: Frequency of backward trajectories for different starting depths ('destination points') on the transect for the years 2008 to 2012 per histogram bin size, see bottom right plot for bathymetry contour lines: green (200 meters), red (500 meters) and black (1000 meters); purple arrows for better visibility of abbreviations (see also Fig. 2) and not necessarily indicating flow direction

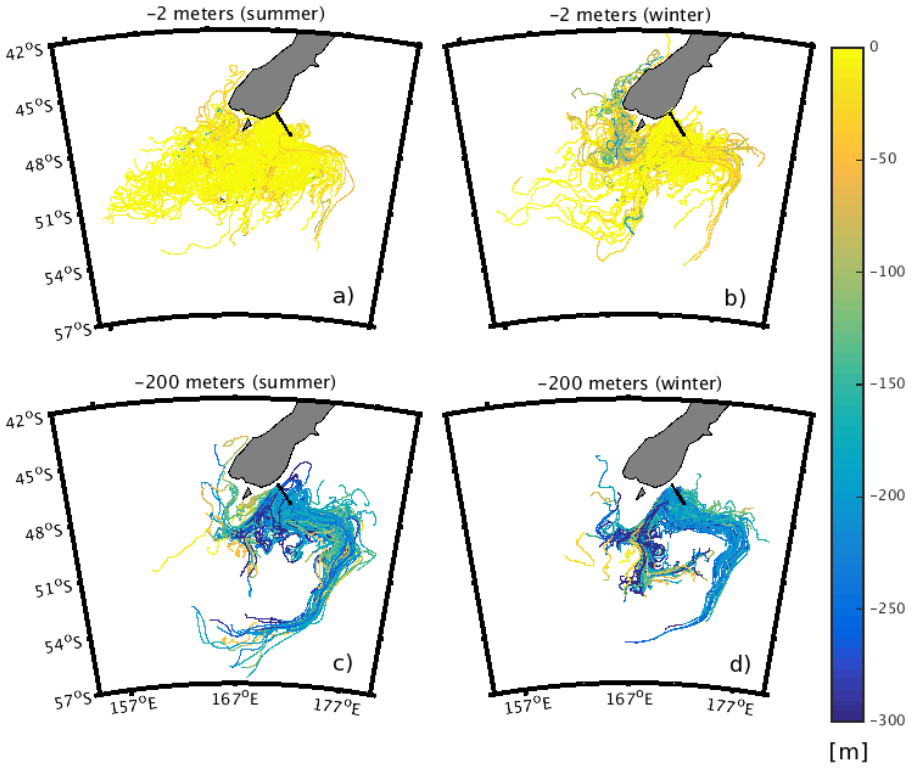


Figure 12: Backward trajectories for summer (left; a & c) and winter (right; b & d) for 2 meters starting depth (top; a & b) and 200 meters starting depth (bottom; c & d) on the SC; colors represent trajectory depth; for better visibility shown trajectories belong exemplarily to year 2008 (other years show similar behavior); each trajectory represents 70 days; for bathymetry contour lines see Fig. 11 right bottom

got already into contact with the atmosphere, freshwater input by New Zealand rivers or mixing. Thus, in this study, the 'earliest' point of time (regarding reality) in the simulation, which corresponds to the source points, is taken to analyze the water parcel origin in terms of its salinity (S) and temperature (T) properties. The S and T information are taken from the source points and thus the last time step of the backwards calculation after (which corresponds in reality to before) 70 days. The location of the water parcel at that point of time (longitude, latitude, depth) is used to extract the S and T properties from the model simulation. This is done for each simulated tracer for all SC section depths. An overview of the properties of the source water masses is given in Fig. 13. The black rectangle illustrates the applied definition of subtropical (STW) and Subantarctic (SAW) water masses based on the salinity-temperature properties of this study and on information given in Smith et al. (2013). In general, south of New Zealand different water masses are known to exist: Neritic Water (NW), Subtropical Water (STW), Subantarctic Surface Water (SASW), Subantarctic Mode Water (SAMW) and Antarctic Intermediate Water (AAIW) (Smith et al., 2013, for instance). In this study, all of those mentioned Antarctic water masses are summarized in the SAW, defined by all water colder than 9 °C or fresher than 34.6 whereas STW is defined as all water warmer than 9 °C and saltier than 34.6. The NW, which is a relatively warm and fresh water mass, cannot explicitly be found in Fig. 13. Generally, NW origins from warm and salty STW that is modified by freshwater outflow from south-west New Zealand (Butler et al., 1992). In Fig. 13 only the source points of the back-trajectories are included to avoid effects of mixing or freshwater inflow on the way for an investigation of the source water masses. Additionally, source points are not frequently located at the south-west coast of New Zealand and if so (during winter, as explained above), they originate from deeper areas and thus are assumed to be rather separated from areas of freshwater input at the surface.

In general, both water mass types (SAW and STW) can be found as source water masses down to about 400 meter depth of destination points, with a main influence of SAW in all depths. All water parcels with destination points beyond that depth downwards to the bottom only originate from Subantarctic waters. The deeper the water parcel reaches the SC the less influence of STW can be found.

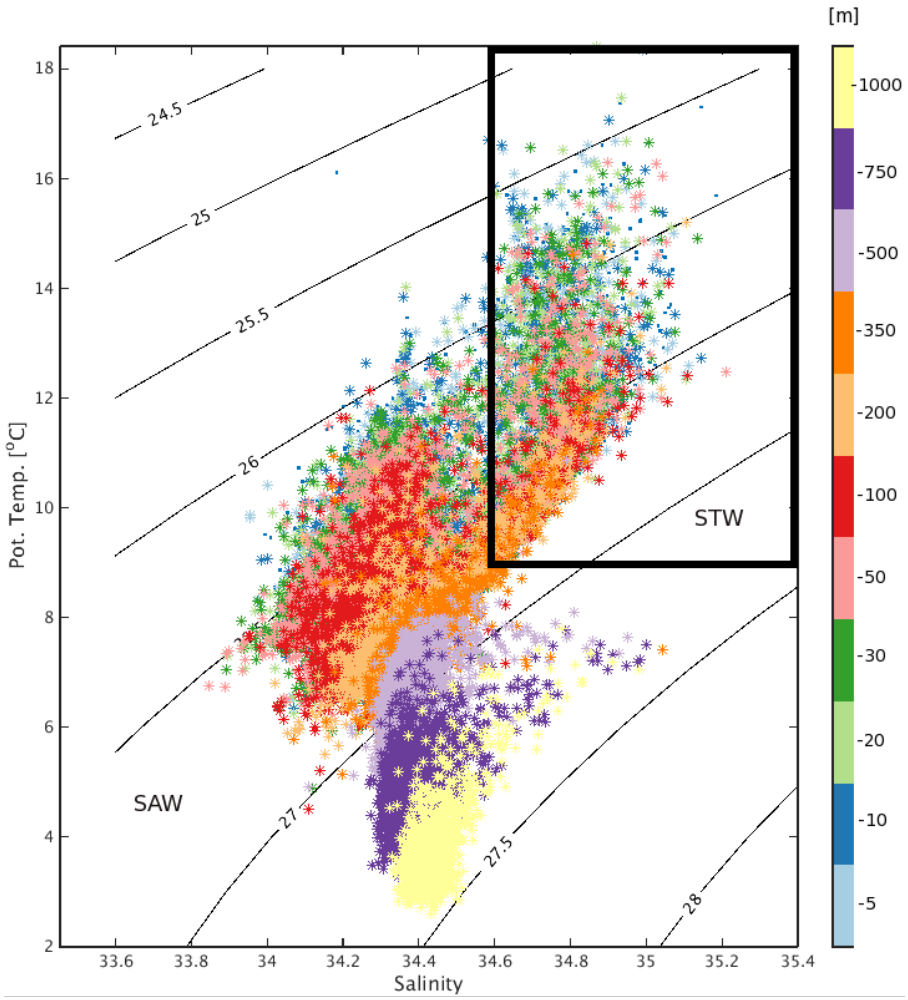


Figure 13: Temperature and salinity information for all back-trajectories at the source points after 70 days of simulation (in reality 70 days before reaching the SC section) to define the source water masses; colors represent the different starting depths on the SC section; definition of Subtropical (STW) and Subantarctic (SAW) waters based on Smith et al. (2013); black lines for density information

To combine the spatial information from Fig. 11 and the source water mass information from Fig. 13, Fig. 14 identifies from which location which source water mass originates. A main separation can be identified: whereas STW (red) originates mainly from the north and from the east, SAW (blue) is mainly transported from the south but also from the east. In shallower water depths of destination points, up to about 200 meters, a clear separation of STW and SAW can be seen around 48 °S, following a curvy u-shape. The water coming from the south-west coast of New Zealand can be completely associated with STW whereas water coming from the east or south but also from south of

about 50 °S can be fully classified as Antarctic and Subantarctic water (SAW).

The Tab. 2 gives an overview of the percentage of STW and SAW at the source points depending on the depths of destination points across the SC section. The results support the observation from before: the deeper the starting depths, the more SAW and the less STW are forming the SC . From about 500 meters downwards, the water ending in the SC section consists of 100 % SAW and no STW can be found anymore. The total amount of STW and SAW is additionally calculated in a further simulation with vertically equally distributed tracers every 100 meters depth from the surface (2 meters) down to the bottom (1300 meters) of the same SC section as before. From these in total 33292 simulated tracers during the 5 years, 95.6 % can be associated with SAW while only 4.4 % have a Subtropical origin (STW).

Table 2: Percentage of source water masses (SAW and STW) that form the SC in a certain depth; calculated by using the endpoint T / S information of all tracers; for the calculation of the total numbers a simulation of equally distributed tracers every 100 meters depth from 2 meters (surface) to 1300 meters (bottom) is used

| Depth [m] | -2 | -5 | -10 | -20 | -30 | -50 | -100 | -200 | -350 | -500 | -750 | -1000 | total |
|---|---|---|---|---|---|---|---|---|---|---|---|---|---|
| STW [%] | 27.5 | 22.6 | 19.4 | 17.3 | 15.7 | 14.9 | 7.8 | 5.9 | 2.0 | 0.0 | 0.0 | 0.0 | 4.4 |
| SAW [%] | 72.5 | 77.4 | 80.6 | 82.7 | 84.3 | 85.1 | 92.2 | 94.1 | 98.0 | 100.0 | 100.0 | 100.0 | 95.6 |
| tot. traj. | 3328 | 3480 | 3584 | 3604 | 3611 | 3586 | 3317 | 3318 | 3228 | 2902 | 2401 | 1697 | 33292 |

# 4 Discussion

## 4.1 Validation

As illustrated in Fig. 10, decreasing $s$-values can be found with increasing length of the simulation. This stands for an 'increased simulation quality' as defined by the resulting increasing $ss$-values, calculated as being relative to the pathway length (see Sec. 2.4). 1 to 5 days after the tracer release, a number of lower quality simulations can be found as illustrated by $s \geq 1$. As consequence, the frequency of occurrence of higher quality simulations ($s < 1$) is lowered compared to longer simulations. This

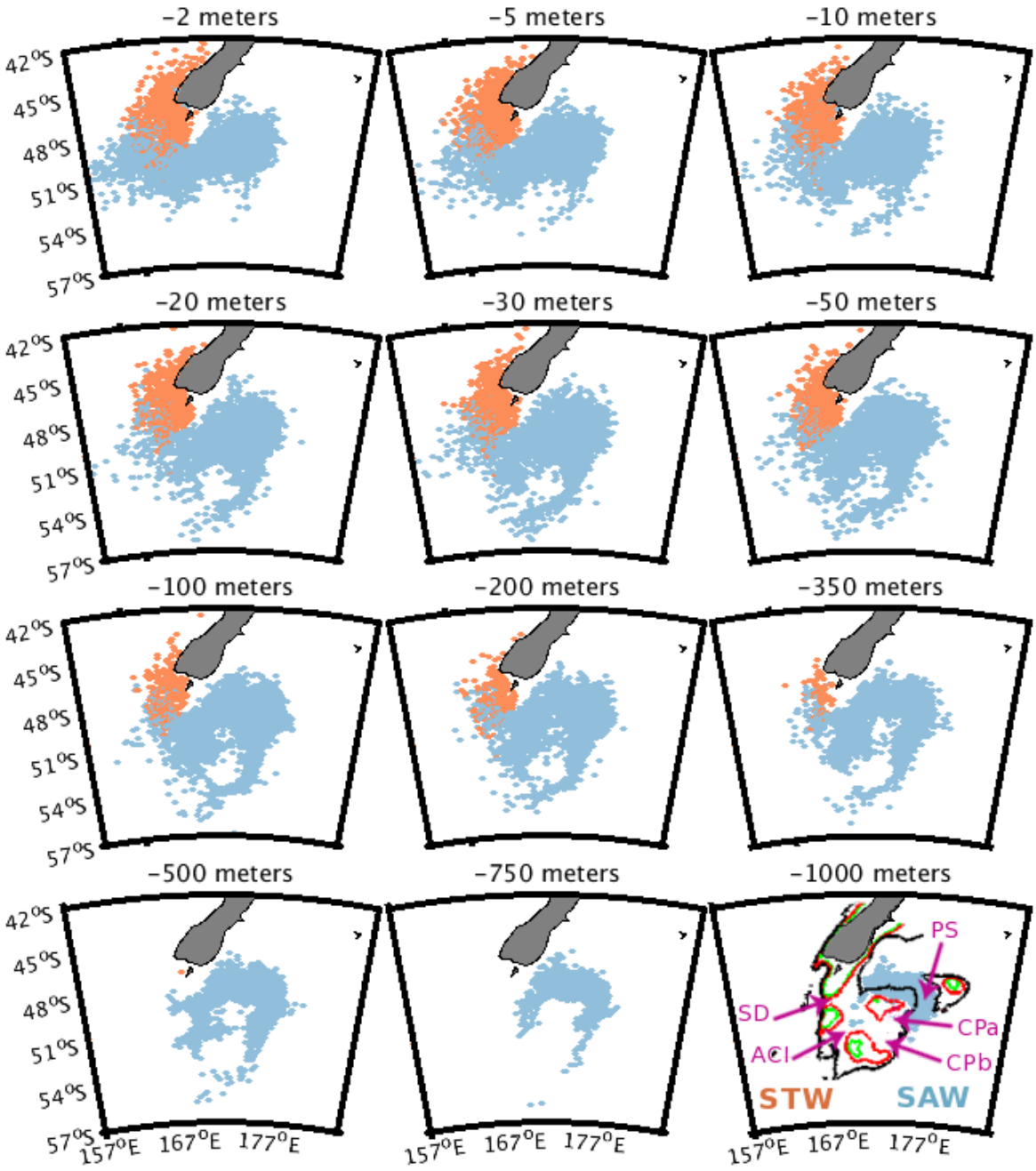


Figure 14: Endpoints of backward trajectories ('source points') after 70 simulation days for different depths of destination points on the SC transect for the years 2008 to 2012 and their corresponding temperature and salinity information to define source water masses (SAW blue and STW red) based on information given by Smith et al. (2013); see bottom right plot for bathymetry contour lines: green (200 meters), red (500 meters) and black (1000 meters); purple arrows for better visibility of abbreviations (see also Fig. 2) and not necessarily indicating flow direction

can be explained by the difficulties within the ROMS simulation to simulate short-term small-scale features as eddies in the way they can be observed in reality. If the TracPy drifter, for instance, is placed inside of an in reality occurring eddy structure directly at the beginning of a simulation, it may happen, that, within the first days, the TracPy drifter and the GDP drifter even travel into completely opposite directions. As a result, the short-term simulation does not match the short-term observation. This is different for longer term simulations. Even if eddies occur on the pathway, the travel-time through such an eddy is comparatively short compared to the overall simulation. The general direction and pathway of the tracers may match although small-scale differences occur. In this study, the aim is to define the water mass composition and origin of the Southland Current. Thus, the study rather focuses on larger-scale structures. Liu and Weisberg (2011) applied their validation method for HYCOM simulation results in the Gulf of Mexico region. They define 'larger skill scores' as scores between 0.5 and 0.9. In the simulation of this study, the threshold of 0.5 is already reached from 16 days after release onwards. In contrast, Liu and Weisberg (2011) define 'smaller skill scores' as values below 0.2 and their mean skill score value for the 3-day simulation period is 0.33, which can even be slightly exceeded by the results of the simulation of this study ($ss_{03} = 0.36$). In this context, the model performance in general, but in particular for the longer-term simulations ($\geq$ 16 days) is considered to be appropriate for the aim of this study.

## 4.2 Backward trajectories and water mass origin

The features of the overall backward trajectories during the entire year (Fig. 11) suggest two different mechanisms:

In the surface layers down to destinations points of about 20 meters depth, the first mechanism is the mainly wind driven general circulation in that region. Water is transported from the west to the east in those latitudes by a strong persistent wind field. Adjacent to the Subtropical Front (STF) the Antarctic Circumpolar Current (ACC) can be found, a strong eastward-directed and persistent current which extends around the entire globe, driven by the world's strongest westerlies at approximately 45

°S - 55 °S (Trenberth et al., 1990, Orsi et al., 1995). In the first of the two acting mechanisms for the trajectory pathways, the surface waters are influenced in the same way and follow an eastwards motion. As a result, surface back-trajectories travel relatively straight and far to the west in the backwards simulation (see Fig. 11 or Fig. 12 a). In addition to the influence of winds and background circulation, the second mechanism to form the trajectory pathways is the influence of local bathymetry. The three mentioned general entrances of water masses can be associated with the Snares Depression (entrance SD), the depression between the Auckland Islands and the Campbell Islands (entrance ACI) and the most southern extent of the Bounty Trough (entrance PS). The mentioned yellow u-shaped trajectories in Fig. 11 result from an increased occurrence of trajectories traveling around the Snares Shelf through the Snares Depression. Regarding those two mechanisms that influence the pathways reaching the SC in the surface layers (the general eastwards background current driven by large-scale wind fields and the bathymetry), results show a main influence of the wind field and the general eastwards directed circulation during summer, and in contrast a notable effect of the local bathymetry during winter. This effect of bathymetry on those winter trajectories is driven by upwelling of water parcels east of the Snares Shelf from about 150 meters, driven by strong winds in autumn and winter (Fig. 12 b). In this depth, water parcels are forced to travel around the Snares Shelf as their pathways are blocked straight to the east by the Snares Shelf. They are forced to enter the Snares Depression from the north as they are additionally blocked from the west by the Macquarie Ridge Complex. Thus, water parcels in that depth have to follow the trench from the north and thus originate from the south-west coast of New Zealand. As a result, it can be assumed that an increased number of water parcels, that are found in the surface layers of the SC transect during winter time, originate from deeper STW near the south-western coastline of New Zealand. These findings of differences during winter and summer are a combination of two different views discussed in literature: Authors either state that SC waters do not appear inshore near the west coast of New Zealand but are more likely advected zonally across the Tasman Sea (e.g. Chiswell, 1996) or authors state that SC waters in general origin from the south-westwards flow at the south-west coast of New Zealand, when this water

flows around the south of the south island and then up the east coast (Heath et al., 1975, Stanton, 1976).

Generally, for water parcels that reach the SC in deeper layers, bathymetry is the mainly controlling factor for resulting pathways and the deeper the water parcels, the stronger the influence of bathymetry on the pathways as water parcels are forced to travel around those features. Comparing the water parcels that reach the SC in deeper layers (Fig. 12 c & d) the major differences can be explained as follows: during summer (Fig. 12 c), when the stratification is still present and thus a thinner SML exists, the deeper water masses, originating from Antarctic water masses, are rather separated due to stratification from the upper layers and thus are not mixed with the upper water. As a result, the deeper layers still carry their original salinity and temperature properties and thus tend to be denser compared to the situation in winter time (Fig. 12 d), when strong mixing occurs which modifies the water masses. The denser water masses in the deeper layers during summer (Fig. 12 c) are therefore forced to mainly travel around the Campbell Plateau (entrance PS in Fig. 2). During winter, this water is modified, resulting in a slightly decreased density. Thus, consisting of those modified properties and well mixed, the water with Antarctic origin may enter the Campbell Plateau already at entrances CPa and CPb in Fig. 2 and thus separates into two pathways: one pathway across the Campbell Plateau (entrances CPa and b) and one pathway, as during summer, through the southernmost part of the Bounty Trough (entrance PS). One assumption for the shorter and thus slower backward trajectories in winter could be the result of this separation: As the water body splits under that condition into several pathways, the water parcels may travel with less pressure and thus less speed. Another explanation for the different travel speed during the seasons could be the seasonal variability in larger-scale circulation features, like the ACC or the Subantarctic Front (SAF). Anyway, the differences in the strength of the currents of this study agree with the results of Stanton and Morris (2004), who describe much weaker flows over the Campbell Plateau compared to the higher flow velocities around the plateau from the Subantarctic Slope southwards, which can be associated with the core of the SAF.

The general transport of the Antarctic water is associated with the ACC and mainly located too far southwards to enter the Campbell Plateau already from the west, where it is mainly blocked by the Macquarrie Ridge Complex. For this reason, only occasionally trajectories with Antarctic origin enter the Campbell Plateau directly from the west in deeper layers. It is known, that the SAF, which is associated with the ACC, consists of three branches (e.g. Rintoul and Bullister, 1999 or Orsi et al., 1995). The northern branch of the SAF is known to directly follow the edge of the Campbell Plateau and thus is assumed to be the most important one in this study. The middle and southern branches are known to turn sharply to the south east of 165 ° E (Sokolov and Rintoul, 2007). A change or variation in the position of the branches of the SAF, in particular of the northern one, may therefore also influence the development of the SC and the composition of involved water masses. Nevertheless, it should be considered that this study is only to a limited degree capable to explain the general circulation pattern around New Zealand. It is rather intended to focus on the source points of the SC and involved water parcel pathways and source water masses. Thus, even if the results of this study do not indicate trajectories via a particular pathway, a flow along this pathway cannot be excluded. Instead, this circumstance rather suggests there is now flow along this pathway contributing to a certain location of the SC at a certain point of time. Water parcels could end up somewhere close to the SC section or could be trapped in eddies for a while before reaching the SC, for instance, while nevertheless traveling along this particular pathway.

Investigating the water masses closer which enter via entrances CPa and b, it can be found, that this water mainly consist of a rather lighter and modified water mass (4 ° C $<$ T $<$ 9 °C; 34.4 $<$ S $<$ 34.6), most likely due to mixing. This is in contrast to the very cold ($<$ 4 °C) or fresh ($<$ 34.4) water masses, which form the main part of the deeper Antarctic water in summer, when it is not able to enter the Campbell Plateau but is forced to travel around the plateau. Generally, the process of a development of an intermediate water layer with modified properties due to strong turbulence at the Subantarctic Front during winter is already known. For example Ivanov et al. (2006) state, this intermediate water layer is formed by sinking of surface waters down to intermediate depths due to

turbulence. Similar processes can be assumed here during winter when the slightly lighter, modified water is capable to enter the Campbell Plateau via entrance CPa and CPb. The surface mixed layer during winter over the Campbell Plateau can easily achieve 300 meters depth (Morris et al., 2001) and deep active mixing in places over the plateau from the surface to the bottom can occur. It has been previously investigated, that strong mixing and convection are capable to generate an Antarctic water mass of almost uniform properties (and thus a minimum stratification) from the surface down to 600 meters, the Subantarctic Mode Water (SAMW) (e.g. Heath, 1981). The SAMW near New Zealand is defined in literature by properties of T $<$ 8 °C and S $<$ 34.45, or over the plateau by T = 7 ° C and S = 34.51 - 34.66, which matches the temperature and salinity ranges of the water mass entering the Campbell Plateau during winter in this study, as mentioned before.

The total amount of Antarctic waters forming the SC (Tab. 2) of about 96% corresponds well to the findings of Sutton (2003). In that study, the author defined the STW and SAW amounts by measurements on several sections across the SC. The two most southern sections can be defined as equivalent to the section in this study. Sutton (2003) presents a SAW amount of about 93 - 98 % in that region, which had been in contrast to previous studies defining the SC as a current mainly originating from Subtropical waters (e.g. Jillett, 1969, Heath et al., 1975). The present study supports the findings of Sutton (2003), defining Antarctic waters as the main source of the SC .

## 5 Summary and conclusion

In this study, ROMS ocean velocity fields for the years 2008 - 2012 are used to force the trajectory model TracPy. A successful validation is presented, comparing ROMS surface temperatures with satellite data, ROMS salinities with climatological data and TracPy trajectories with drifter data. Already for simulations of 16 days, the drifter validation shows a mean skill score of $mss \geq 0.5$, which is defined in literature as 'larger skill score' (whereas 'smaller skill scores' are defined in literature as $ss$

$< 0.2$). Based on the validation results, the skill score is expected to further increase with simulation length.

Afterwards, TracPy backward trajectory simulations for the period 2008 - 2012 are conducted. Tracers are placed across the Southland Current (SC) section in several depths and are calculated 70 days backwards in time. Results are analyzed regarding the entire trajectory pathways as well as regarding the source water masses at the endpoints of the trajectories ('source points') to define origin and formation of the SC .

Results indicate a different formation of the SC for different seasons: Water parcels that reach the SC in surface layers either origin from surface waters mainly from the west without being influenced by local bathymetry (summer situation) or origin from deeper layers at the south-west coast of New Zealand, following the local bathymetry around the Snares Shelf (winter situation). The winter situation is assumed to occur due to stronger winds that generates upwelling at the eastern side of the Snares Shelf whereas water parcels during summer mainly follow the present eastwards oriented background current. These findings reconcile previous contradictory studies, that either state an origin of the SC by a zonal advection across the Tasman Sea as SC waters are not found on the west coast of New Zealand or state that water from the west coast flows around Steward Island to appear at the east coast in the SC . Water parcels that reach the SC in deeper layers are always influenced by local bathymetry on their way into the SC but also in a different way during different seasons: During summer, these water parcels mainly follow the current around the Campbell Plateau whereas during winter, an increased amount of these water parcels enters the Campbell Plateau and travels across the plateau before entering the SC . This could be a result of increased mixing and convection during winter, followed by the development of a very deep mixed layer and a slightly lighter water mass (as Subantarctic Mode Water, SAMW) so that the water is able to enter the eastern side of the plateau, or a result of changes in larger-scale features (as the ACC or the STF). Nevertheless, the application of backward trajectories as in this study is not suitable to explain the general circulation pattern around New Zealand but can only give insights regarding the formation and sources of the SC at a certain

point of time. Oceanic currents could generally be oriented in a similar way during different seasons but without contributing to the SC . This could happen when water parcels are trapped for a while in eddies at a certain location or when parcels traveled similar pathways but end somewhere close to the SC but not inside.

Results of this study regarding the amount of Subtropical (of about 4 %) and Subantarctic (of about 96 %) waters forming the SC support more recent studies, disagreeing with previous studies that stated the SC is mainly of tropical origin.

These differences in the origin as well as the pathways of water masses forming the SC surface layers may provide valuable information for further studies, for instance regarding the location of the STF and its variability, as previous studies are discussing whether the STF is located around or across the Snares Shelf (Smith et al., 2013). It could also provide information for studies focusing on surface measurements across the SC, as $CO_2$ measurements similar to Currie et al. (2009) for instance, as it implies differences in the time, duration and location of ocean-atmosphere exchange during different seasons.

# 6 Acknowledgments

We would like to thank the International Research Training Group INTERCOAST and the Deutsche Forschungsgemeinschaft (DFG) for funding for this study.

Cape Saunders ADCP data were collected by MetOcean Solutions Ltd under contract to OMV New Zealand Ltd and remain the property of OMV. The authors would like to thank both parties for their permission to use the data.

Many thanks for interesting and valuable discussions to P. Sutton, G. Rickard and S. Chiswell and also for the possibility to visit and work at NIWA Wellington during a part of this study.

## References


Barron, C. N., Smedstad, L. F., Dastugue, J. M., and Smedstad, O. M. (2007). Evaluation of ocean models using observed and simulated drifter trajectories: Impact of sea surface height on synthetic profiles for data assimilation. *Journal of Geophysical Research: Oceans*, 112(C7). C07019.

Blanke, B. and Raynaud, S. (1997). Kinematics of the Pacific Equatorial Undercurrent: an Eulerian and Lagrangian approach from GCM results. *Journal of Physical Oceanography*, (27):1038–1053.

Butler, E. C. V., Butt, J. A., Lindstrom, E., Teldesley, P., Pickmere, S., and Vincent, W. (1992). Oceanography of the Subtropical Convergence Zone around southern New Zealand. *New Zealand Journal of Marine and Freshwater Research*, 26(2):131–154.

Chiswell, S. M. (1996). Variability in the Southland Current, New Zealand. *New Zealand Journal of Marine and Freshwater Research*, 30(1):1–17.

Chiswell, S. M., Bostock, H. C., Sutton, P. J. H., and Williams, M. J. (2015). Physical oceanography of the deep seas around New Zealand: a review. *New Zealand Journal of Marine and Freshwater Research*, 49-2:286–317.

Currie, K. I., Reid, M. R., and Hunter, K. A. (2009). Interannual variability of carbon dioxide drawdown by Subantarctic surface water near New Zealand. *Biogeochemistry*, 104(1):23–34.

Döös, K. (1995). Interocean exchange of water masses. *Journal of Geophysical Research: Oceans*, 100(C7):13499–13514.

Döös, K., Rupolo, V., and Brodeau, L. (2011). Dispersion of surface drifters and model-simulated trajectories. *Ocean Modelling*, 39(34):301–310.

Dunn, J. and Ridgway, K. (2002). Mapping ocean properties in regions of complex topography. *Deep Sea Research Part I: Oceanographic Research Papers*, 49(3):591–604.

Fernandez, D. (2016). *Variability, coherence and forcing mechanisms in the New Zealand ocean boundary currents*. PhD thesis, The University of Auckland, New Zealand.

Greig, M. J. and Gilmour, A. E. (1992). Flow through the Mernoo Saddle, New Zealand. *New Zealand Journal of Marine and Freshwater Research*, (26:2):155–165.

Haidvogel, D., Arango, H., Budgell, W., Cornuelle, B., Curchitser, E., Lorenzo, E. D., Fennel, K., Geyer, W., Hermann, A., Lanerolle, L., Levin, J., McWilliams, J., Miller, A., Moore, A., Powell, T., Shchepetkin, A., Sherwood, C., Signell, R., Warner, J., and Wilkin, J. (2008). Ocean forecasting in terrain-following coordinates: Formulation and skill assessment of the regional ocean modeling system. *Journal of Computational Physics*, 227(7):3595–3624. Predicting weather, climate and extreme events.

Heath, R. (1981). Oceanic fronts around southern New Zealand. *Deep Sea Research Part A. Oceanographic Research Papers*, 28(6):547–560.

Heath, R. A., of Scientific, N. Z. D., and Research, I. (1975). *Oceanic circulation and hydrology off the southern half of South Island, New Zealand*. Wellington: New Zealand Oceanographic Institute. At head of title: New Zealand Department of Scientific and Industrial Research.

Ivanov, Y. A., Anisimov, M. V., and Subbotina, M. M. (2006). Seasonal variability of the water circulation in the southern ocean and heat, salt, and mass exchange in the Antarctic region and adjacent oceans. *Oceanology*, 46(4):453–464.

Jillett, J. B. (1969). Seasonal hydrology of waters off the Otago peninsula, South-Eastern New Zealand. *New Zealand Journal of Marine and Freshwater Research*, 3(3):349–375.

Kalnay, E., Kanamitsu, M., Kistler, R., Collins, W., Deaven, D., Gandin, L., Iredell, M., Saha, S., White, G., Woollen, J., Zhu, Y., Leetmaa, A., Reynolds, R., Chelliah, M., Ebisuzaki, W., Higgins, W., Janowiak, J., Mo, K., Ropelewski, C., Wang, J., Jenne, R., and Joseph, D. (1996). The

ncep/ncar 40-year reanalysis project. *Bulletin of the American Meteorological Society*, 77(3):437–471.

Liu, Y. and Weisberg, R. H. (2011). Evaluation of trajectory modeling in different dynamic regions using normalized cumulative Lagrangian separation. *Journal of Geophysical Research: Oceans*, 116(C9). C09013.

Lumpkin, R. and Pazos, M. (2007). Measuring surface currents with surface velocity program drifters: the instrument, its data, and some recent results. pages 39–67. Cambridge Books Online.

Marchesiello, P., McWilliams, J., and Shchepetkin, A. (2001). Open boundary conditions for long-term integration of regional oceanic models. *Ocean Modelling*, 3(1-2):1–20.

Morris, M., Stanton, B., and Neil, H. (2001). Subantarctic oceanography around New Zealand: Preliminary results from an ongoing survey. *New Zealand Journal of Marine and Freshwater Research*, 35(3):499–519.

Oezgoekmen, T., Griffa, A., Mariano, A., and Piterbarg, L. I. (2000). On the Predictability of Lagrangian Trajectories in the Ocean. *Journal of Atmospheric Oceanic Technology*, 17:366–383.

Orsi, A. H., Whitworth, T., and Nowlin, W. D. (1995). On the meridional extent and fronts of the Antarctic Circumpolar Current . *Deep Sea Research Part I: Oceanographic Research Papers*, 42(5):641–673.

Paldor, N., Dvorkin, Y., Mariano, A. J., Oezgoekmen, T., and Ryan, E. H. (2004). A practical, hybrid model for predicting the trajectories of near-surface ocean drifters. *Journal of Atmospheric Oceanic Technology*, 21:1246–1258.

Pazos, M. (2015). All you wanted to know about drifters. Technical report, Drifter Data Assembly Center NOAA/ AOML, Miami, Florida.

Preisendorfer, R. (1988). Principal component analysis in meteorology and oceanography. *Elsevier*.

Price, J. M., Reed, M., Howard, M. K., Johnson, W. R., Ji, Z.-G., Marshall, C. F., Jr., N. L. G., and Rainey, G. B. (2006). Preliminary assessment of an oil-spill trajectory model using satellite-tracked, oil-spill-simulating drifters. *Environmental Modelling & Software*, 21(2):258–270. Progress in Marine Environmental ModellingProgress in Marine Environmental Modelling.

Reynolds, R. W., Smith, T. M., Liu, C., Chelton, D. B., Casey, K. S., and Schlax, M. G. (2007). Daily high-resolution-blended analyses for sea surface temperature. *Journal of Climate*, (20):5473–5496.

Ridgway, K. R., Dunn, I. R., and Wilkin, I. (2002). Ocean interpolation by four-dimensional weighted least squares application to the waters around Australasia. *Journal of Atmospheric Oceanic Technology*, 19:1357–1375.

Rintoul, S. R. and Bullister, J. L. (1999). A late winter hydrographic section from Tasmania to Antarctica . *Deep Sea Research Part I: Oceanographic Research Papers*, 46(8):1417 – 1454.

Shchepetkin, A. F. and McWilliams, J. C. (2005). The regional oceanic modeling system (ROMS): a split-explicit, free-surface, topography-following-coordinate oceanic model . *Ocean Modelling*, 9(4):347–404.

Smith, R. O., Vennell, R., Bostock, H. C., and Williams, M. J. (2013). Interaction of the subtropical front with topography around southern New Zealand. *Deep Sea Research Part I: Oceanographic Research Papers*, 76:13–26.

Smith, S. (1988). Coefficients for sea surface wind stress, heat flux, and wind profiles as a function of wind speed and temperature. *Journal of Geophysical Research*, 93(C12):15467–15472.

Sokolov, S. and Rintoul, S. R. (2007). Multiple Jets of the Antarctic Circumpolar Current South of Australia. *Journal of Physical Oceanography*, 37(5):1394–1412.

Stanton, B. R. (1976). Circulation and hydrology off the west coast of the South Island, New Zealand. *New Zealand Journal of Marine and Freshwater Research*, 10(3):445–467.

Stanton, B. R. and Morris, M. Y. (2004). Direct velocity measurements in the subantarctic front and over campbell plateau, southeast of new zealand. *Journal of Geophysical Research: Oceans*, 109(C1). C01028.

Sutton, P. J. H. (2003). The Southland Current A subantarctic current. *New Zealand Journal of Marine and Freshwater Research*, 37(3):645–652.

Thompson, R. (1983). Low-pass filters to suppress inertial and tidal frequencies. *Journal of Physical Oceanography*, 13(6):1077–1083.

Thyng, K. M. and Hetland, R. D. (2014). TracPy: Wrapping the Fortran Lagrangian trajectory model TRACMASS. Technical report, Texas A&M University.

Trenberth, K. E., Large, W. G., and Olson, J. G. (1990). The mean annual cycle in global ocean wind stress. *Journal of Physical Oceanography*, 20(11):1742–1760.

Uddstrom, M. J. and Oien, N. A. (1999). On the use of high-resolution satellite data to describe the spatial and temporal variability of sea surface temperatures in the New Zealand region. *Journal of Geophysical Research: Oceans*, 104(C9):20729–20751.

Vries, P. and Döös, K. (2001). Calculating Lagrangian trajectories using time-dependent velocity fields. *Journal of Atmospheric Oceanic Technology*, 18:1092–1101.